Correlating Molecular Design to Microstructure in Thermally Convertible Oligothiophenes: The Effect of Branched versus Linear End Groups

Dean M. DeLongchamp,*,† Youngsuk Jung,† Daniel A. Fischer,† Eric K. Lin,† Paul Chang,‡ Vivek Subramanian,‡,§ Amanda R. Murphy,§,|| and Jean M. J. Fréchet§,||

Materials Science and Engineering Laboratory, National Institute of Standards and Technology, Gaithersburg, Maryland 20899, Department of Electrical Engineering and Computer Sciences and Department of Chemistry, University of California, Berkeley, California 94720, and Division of Materials Science, Lawrence Berkeley National Laboratory, Berkeley, California 94720

Received: January 31, 2006; In Final Form: April 3, 2006

The thin film microstructure development of functionalized oligothiophenes with branched, thermally removable groups at each end of conjugated cores with five, six, and seven thiophene rings was monitored during their thermal conversion from solution processible precursors to insoluble semiconductor products. The change in end group character provides a comparison of branched vs linear end group functionalization in oligothiophenes. Near edge X-ray absorption fine structure (NEXAFS) spectroscopy confirmed that branched α-, ω-substitutions of the precursors strongly influenced the packing of the conjugated core. The quinque- and sexithiophene precursors oriented perpendicular to the substrate, whereas the septithiophene precursor oriented parallel to the substrate, providing one of the first examples of length dependence in oligothiophene orientation. This dependence may be due to a packing mismatch between the conjugated cores and the branched end groups. The convertible septithiophene exhibits four distinct microstructures as it converts from precursor to product that correlate strongly with its field-effect hole mobility in field-effect transistors. The extent of septithiophene order and the surface-relative orientation of its ordered phases clearly influence field-effect transistor performance.

Introduction

Organic semiconductors enable new applications and new modes of device production because they can be applied from vapors or solutions to form flexible films. Within these films, conjugated semiconducting molecules can form a microstructure where the prevalence of crystals, their size, and their molecular orientation can influence hole or electron transport.[1−3] The most desirable processing technique for organic semiconductors is solution deposition, where the microstructure of the film is formed during the dynamic assembly of molecules into a solid. This assembly process is influenced by factors including the substrate chemistry,[4−8] substrate temperature,[4,9−13] and the rate of solvent removal if it is present.[7,14] However, the most important factor governing microstructure development is the primary chemical structure of the organic semiconductor, because the strength and geometry of intermolecular interactions provide the driving force for crystallization. The strong influence of chemical structure has prompted much work in the molecular design of organic semiconductors, where variations in crystallinity, packing style, and molecular orientation have been successfully controlled by directed functionalization.[15−19] The oligothiophenes and oligoacenes have proven to be useful starting motifs for developing guidelines for molecular design.

Recently, we introduced a new class of oligothiophenes designed with a precursor conversion strategy to facilitate processing.[20,21] The precursors are oligothiophenes substituted at the terminal α and ω positions with branched activated esters. These precursors can be dissolved in common solvents such as chloroform, cast or printed,[22] and then heated to remove the solubilizing ester end groups. The products of this conversion provide high hole mobility in field-effect transistors (FETs), compared to other solution processed oligothiophenes. The molecular structures of precursors and products are shown in Figure 1. Soluble precursors provide a useful platform for studying the effects of molecular design on microstructure because the precursors are substituted with branched end groups, whereas the products are substituted with small, linear allyl groups. We exploit this changing end group character to develop a comparison of branched vs linear end group functionalization in oligothiophenes. Microstructure development is characterized over the thermal conversion from precursor to product for convertible oligothiophenes with five, six, and seven thiophene rings, enabling the correlation of primary chemical structure to microstructure for six distinct chemical species. Transitions at states of partial conversion are also evaluated.

To characterize thin film microstructure, we use near edge X-ray absorption fine structure (NEXAFS) spectroscopy.[23] Orientation analysis relies on the carbon K-edge, where incident soft X-rays excite carbon 1s electrons to unoccupied σ* and π* molecular orbitals. By changing the incident angle of the linearly polarized soft X-rays and evaluating the angle dependence of certain resonances, the substrate-relative orientation of the conjugated plane and long axis of an oligothiophene core can be determined.[24] The NEXAFS technique does not measure

* Corresponding author. E-mail: deand@nist.gov. Mailing address: Polymers Division, National Institute of Standards and Technology, Gaithersburg, MD 20899-8541.

† National Institute of Standards and Technology.

‡ Department of Electrical Engineering and Computer Sciences, University of Califonia, Berkeley.

§ Lawrence Berkeley National Laboratory.

|| Department of Chemistry, University of Califonia, Berkeley.

10.1021/jp060667t CCC: $33.50
Published on Web 05/17/2006

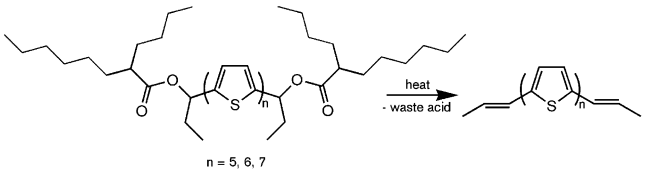

Figure 1. Reaction scheme for the thermally convertible oligothiophenes.

intermolecular arrangement, so it cannot discriminate between packing styles such as the herringbone or cofacial π stack.[18,19] However, NEXAFS measurements can describe the substrate-relative orientation of the oligothiophene long axis and π orbitals in the source-drain plane of organic field-effect transistors (OFETs). This aspect of the crystalline microstructure can be related to the hole or electron transport capability of an organic semiconductor[2,3] and, in some circumstances, can be correlated to the field-effect mobility measured in OFETs.[24]

From studying the microstructure development of convertible oligothiophenes with NEXAFS spectroscopy, we find that the bulky, branched end groups of the precursors strongly influence the packing of the conjugated core, whereas the small allyl end groups of the products do not. These results add to previously described oligothiophene structure−property relationships, where linear α-, ω-substitutions are understood to have almost no influence on the orientation of the conjugated core.[10,25−27] The branched end groups of the precursors studied here cause a very different oligothiophene microstructure than has been previously described and also provide one of the first examples of a dependence of orientation on core length.

Experimental Section

The synthesis and purification of the symmetrical α-, ω-substituted quinque-, sexi-, and septithiophene oligomers (T5, T6, and T7) with thermally removable ester solubilizing groups have been previously described.[20,21] Their primary chemical structures are shown in Figure 1. The purified precursor solids were dissolved at 2−3 mg/mL in anhydrous chloroform (Aldrich). (Certain equipment, instruments, or materials are identified in this paper in order to adequately specify the experimental details. Such identification does not imply recommendation by the National Institute of Standards and Technology, nor does it imply that the materials are necessarily the best available for the purpose.) Films were spun−cast from these solutions onto ozone-cleaned, 105 nm thick SiO_2 that had been thermally grown on highly n-doped (by phosphorus) silicon wafers. A typical precursor film thickness was ≈30 nm as measured by laser ellipsometry. Precursor films were heated on a Brewer Sciences hot plate to temperatures between 50 and 300 °C in a nitrogen atmosphere. The samples were heated for 20 min and then cooled. During conversion, the organic semiconductor autophobically dewetted, resulting in sparse, tall domains separated by low, persistent terraces of 2−3 molecular layers that covered most of the surface area of the SiO_2 dielectric.

NEXAFS spectroscopy was performed at the NIST/Dow soft X-ray materials characterization facility at the National Synchrotron Light Source (NSLS) of Brookhaven National Laboratory. Carbon K-edge partial electron yield (PEY) spectra were collected at a grid bias of −50 V for a surface-weighted sampling depth of ≈6 nm.[6] For PEY spectra, the experimental standard uncertainty of the incident energy is ±0.15 eV, and the yield uncertainly is ±2%. Six peaks were simultaneously fit to the PEY carbon K-edge NEXAFS spectra. A multivariate secant update (More−Hebdon) was used to fit the spectra. Fitted peaks included an error function step convoluted to an exponential decay for the ionization edge, Gaussian peaks before the edge, and asymmetric Gaussian peaks after the edge.[28]

Carbon K-edge NEXAFS spectra were collected for seven incident angles, Θ, from 20° to 70°. Peaks were fit to each of these spectra, and the areas of certain peaks were fit to a trigonometric relationship for an azimuthally averaged surface-relative orientation of the resonances (essentially, a linear fit of peak area vs $\cos^2\Theta$).[23] The two resonances used to find the conjugated core orientation were the carbon−carbon 1s → π^* of the core at 285.4 eV, which defines the conjugated plane (or "ring plane") orientation, and the carbon−carbon 1s → σ^* at 294 eV, which roughly defines the long axis orientation. The actual fits were nonlinear to a dichroic ratio, *R*, which is defined in previous work.[29] The maximum *R* is ≈0.7, which indicates a perfectly edge-on conjugated plane (applied to the π^* resonance) or a horizontal long axis (applied to the σ^* resonance). The minimum *R* is −1.0, which indicates a plane-on conjugated plane or a vertical long axis. A detailed description of experimental and data analysis methods for NEXAFS spectroscopy of organic semiconductors is available elsewhere.[29]

Orientation Trends of Precursors and Products

Trend with Conversion. The first step in correlating orientation with molecular design is attributing orientations to the changing chemical structures of the oligothiophenes during the progression of the conversion reaction. We have previously characterized the thermolysis reaction using a NEXAFS analysis of alkene formation and carbonyl loss as a function of treatment temperature.[20,21] As-cast films of the precursors pre-T5, pre-T6, and pre-T7 exhibit a small amount of end group loss. The precursor films exhibit no further conversion until the treatment temperature exceeds ≈125 °C and end group thermolysis begins. The extent of thermolysis increases from 125 to 225 °C and remains essentially constant at temperatures above 225 °C, as shown in Figure 2c. The apparent reaction rate depends on the oligothiophene core length. The shorter pre-T5 converts to greater extents at lower temperatures than the longer pre-T7. Because the leaving group chemistries are similar for the two oligothiophenes, this difference in reaction rate may be related to differences in molecular motion.[21]

The development of molecular orientation from precursor to product can be followed by quantifying the orientations of key resonances within the NEXAFS spectra.[24,29] Figure 2 shows the long axis (a) and conjugated plane orientations (b) of the conjugated cores, quantified by their dichroic ratios *R*, as they change with temperature. The shortest oligomer, T5, is vertical as-cast, then passes through an isotropic regime at the onset of thermolysis, and finally becomes vertical after full conversion. The intermediate oligomer T6 exhibits similar behavior, with less vertical orientation than pre-T5 in its precursor and a similar orientation to T5 in its product. The longest oligomer T7 exhibits a different behavior, where it is oriented horizontally and plane-on (at 100 °C) before conversion, passes through an isotropic regime, and then assumes a vertical orientation. We consider the pre-T7 orientation at 100 °C to be the precursor equilibrium orientation; the as-cast orientation differs, as we discuss later in this report. The orientation trends in Figure 2a and b are interpreted in Figure 2c with illustrations of the molecular orientation tendency with respect to the substrate plane. In general, the development of orientation proceeds in three stages: (1) the cores are oriented as-cast, (2) they pass through

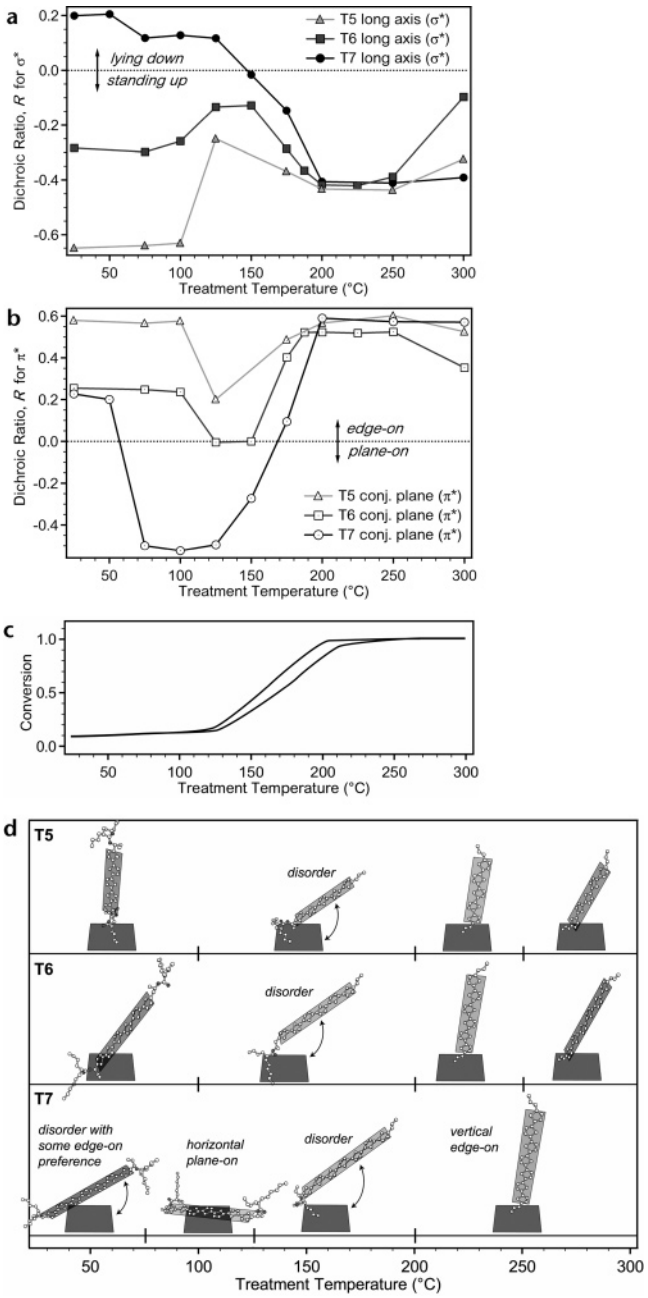

Figure 2. Orientation trends for T5−T7 series with thermal treatment. (a) Trends in the long axis orientation. (b) Trends in the conjugated plane orientation. Typical uncertainty for the orientation measurement R is ±5%. (c) Extent of conversion with temperature. Precursors with smaller cores convert to a greater extent at lower temperatures; the range shown represents all three materials. (d) Illustrated interpretations of the orientations measured in a and b.

an isotropic transition, and (3) they become oriented after conversion. The orientation of the precursors depends on the oligothiophene core length, but the orientation of the products does not.

Trend with Precursor Core Length. The precursor orientation shifts from vertical to horizontal as the oligothiophene core length is increased. This result contrasts with previous reports of α-, ω-substituted oligothiophenes, which describe only a vertical orientation such as that of pre-T5, regardless of core length. Vertical orientation has also been reported for unsubstituted oligothiophenes, such as α-quater-, α-sexi-, and α-octithiophene, which pack in a herringbone arrangement.[30,31] The unusual orientation behavior of these precursors is due to their end groups. Previously reported α-, ω-substituted oligothiophenes featured linear alkyl end groups[10,25−27] (or linear perfluoroalkyl end groups[32]), whereas these precursors have comparatively bulky, branched end groups. These precursors exhibit a new oligothiophene molecular design effect: branched α-, ω-substitution can cause the microstructure to be sensitive to core length and in some cases leads to horizontal, plane-on oligothiophene packing.

The unusual orientation shift of the precursors with core length may be caused by a packing mismatch between the cores and the end groups. In linear α-, ω-alkyl-substituted oligothiophenes, the end groups tilt relative to the vertical conjugated cores to allow the end groups to densely pack without disrupting core−core interactions.[25,26] The branched end groups of the precursors studied here may be too large to allow close core packing. The saturation field-effect hole mobilities of precursor films suggest that there is a shift in the quality of precursor core packing with a changing core length. The vertical phase of pre-T6 exhibits a mobility of $\approx 10^{-4}$ cm^2/(V s),[24] whereas the horizontal, plane-on phase of pre-T7 (after heated to 100 °C) exhibits a mobility of $\approx 10^{-3}$ cm^2/(V s), indicating that the pre-T6 may have frustrated core packing whereas pre-T7 may have closer core packing.

The differences in packing behavior and chemical structure dependence among unsubstituted, linearly end-substituted, and branched end-substituted oligothiophenes may be reconciled by elaborating upon a conceptual model proposed by Garnier et al.[25] In this model, the microstructure is directed by the interplay of two forces: (1) the π affinity of the cores and (2) the segregation of the dissimilar cores and end groups. This model treats the microstructuring of oligothiophenes as a form of self-assembly, where the spatial organization of the crystal lattice is assisted by the thermodynamics of phase segregation at the molecular level. In unsubstituted oligothiophenes, π affinity is the most dominant driving force, and it results in the typical vertical close packing. In linearly substituted oligothiophenes, both π affinity and phase segregation are satisfied by a microstructure where the end chains pack into lamellae that are segregated from the lamellae of vertical close packed cores. The added segregation driving force is believed to cause linearly substituted oligothiophenes to form larger crystals than unsubstituted oligothiophenes.[10,25,27,33]

For branched, end-substituted oligothiophenes, the bulkiness of the aliphatic portion may make simultaneous lamellar segregation and close core packing more difficult. For pre-T5 and pre-T6, the segregation force may be stronger than π affinity, causing the molecules to orient vertically despite poor core packing. However, for pre-T7, the π affinity of the cores may become stronger than the segregation force. The close packed pre-T7 cores may then adopt a horizontal orientation because the end groups prevent close vertical core packing. The shift in precursor orientation with increasing core length may arise from this interplay of π interactions and segregation—in particular the increasing strength of π interactions and their redirection of microstructure despite molecular level phase mixing.

Trend with Product Core Length. In contrast to their precursors, the products T5, T6, and T7 exhibit very similar orientations. The core orientation of the product is consistent with the vertical, lamellar order achieved for unsubstituted or linearly substituted oligothiophenes. There is no dependence of core orientation on whether the core is composed of an odd or even number of thiophene rings. Odd/even effects in unsubstituted[13] and substituted[11] thiophene oligomers have been reported

(the odd oligomers appear to have two crystalline polymorphs), but these differences appear to be substrate temperature dependent[13] and disappear at higher substrate temperatures. Because the products are generated at high substrate temperatures (>200 °C), the odd polymorphs may not appear in these convertible systems. We conclude that the terminal allyl group of the products may be viewed as a short linear substitution, and the microstructure that results is analogous to that of linearly substituted or unsubstituted oligothiophenes.

The product oligothiophenes are similar to previously characterized oligothiophenes, and their orientations determined by NEXAFS spectroscopy can be compared to the orientations of other oligothiophenes that were determined by X-ray diffraction. Most X-ray diffraction investigations of unsubstituted and linearly substituted oligothiophenes report an "essentially vertical" core orientation.[10,31,34] These reports are based on the correspondence of the molecular long axis length with the out-of-plane diffraction spacing. NEXAFS measurements provide independent orientation measurements of the long axis and conjugated plane orientations relative to the substrate. Although the σ^* resonance orientation in Figure 2a is an excellent indicator of trends in long axis orientation, it includes off-axis contributions from the cis nature of the backbone and its orientation is not the molecular orientation. In contrast, the π^* resonance orientation in Figure 2b includes no off-plane contributions. The conjugated plane dichroic ratio R of $\approx$0.6 for the products corresponds to a tilt of the conjugated plane normal of $\approx$78° from surface normal, assuming a single molecular orientation that is azimuthally averaged. This small tilt is consistent with the essentially vertical orientation found for other oligothiophenes by X-ray diffraction. The deviation from a perfect vertical orientation may indicate a slight preferential tilt of the conjugated plane or, more likely, some distribution in orientation due to disordered regions or grain boundaries.

Behavior of T7

Of the convertible oligothiophenes, T7 exhibits the most comprehensive reorientation from precursor to product. This reorientation is highlighted in Figure 3, which shows incident angle-dependent NEXAFS spectra of films before and after conversion. The reversal of conjugated plane orientation is indicated by the change in angle dependence of the two π^* resonances near 285 eV, and the reversal of long axis orientation is indicated by the change in angle dependence of the σ^* resonance at 294 eV. T7 also differs from the shorter convertible oligothiophenes in that the T7 product does not lose its vertical orientation above 250 °C. The vertical orientation of T7 is more stable because it experiences less coverage loss at high temperatures.[21]

The precursor pre-T7 exhibits an orientation transition that is not related to chemistry. The as-cast pre-T7 exhibits a slight tendency toward horizontal, edge-on orientation, but the R values are near zero, indicating that the molecules may be mostly disordered. At temperatures between 75 and 125 °C, pre-T7 assumes a horizontal, plane-on orientation. This second orientation of the precursor is stronger than the as-cast orientation, and it is likely that the material has become significantly more ordered. During casting, pre-T7 may assume a mostly amorphous phase where packing is arrested due to the low molecular diffusivity of pre-T7 and the high volatility of the casting solvent, chloroform. Work with sexithiophene films has shown that kinetically favored phases can be created in a similar way using fast evaporative deposition.[14] Heating above 50 °C must

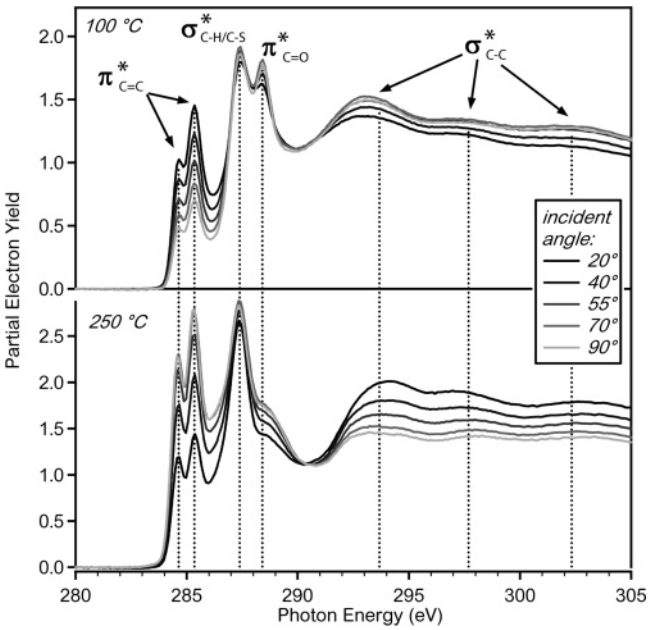

Figure 3. NEXAFS spectra of T7 before and after conversion. The top spectra are for the sample treated at 100 °C, and the bottom spectra are for the sample treated at 250 °C. The uncertainty of the PEY signal is ±2%, and the uncertainty of the photon energy is ±0.15 eV

impart diffusivity to the pre-T7 and allow it to assemble into a more thermodynamically preferred orientation. There is no analogous transition in pre-T5 or pre-T6, possibly because their higher diffusivities allow them to assemble into oriented microstructures before the casting solvent evaporates.

To fully characterize the restructuring of T7, atomic force microscopy (AFM) images were collected for films that had been heated and cooled, as shown in Figure 4. The as-cast films exhibit a grainy texture of soft, unconnected plates with a length scale of 100−200 nm. After heating to 75 °C, the plates fuse into a network of ribbons with a length of 200−400 nm, a width of 40−60 nm, and a height of 10−20 nm. This morphology change of pre-T7 is correlated to its nonchemical orientation transition. The ribbon long axes appear to be oriented predominantly within the substrate plane. Ribbonlike supramolecular organization has been reported for other sexithiophenes that were α-, ω-substituted with chiral penta(ethylene glycol) chains; these molecules formed ribbons that were longer and less branched than those of pre-T7.[35] The dimensions of the pre-T7 ribbons do not correspond to molecular dimensions, and the molecular orientation cannot be directly determined from the AFM images. However, the NEXAFS measurement indicates that the septithiophene conjugated plane normal is oriented perpendicular to the long axes of the ribbons (and perpendicular to the surface), not parallel to them as is typical for rods or ribbons of conjugated molecules.[35−37] The ribbons become soft terraces midway through conversion at 175 °C and, finally, become sharp terraces after full conversion. The terrace height corresponds well to the $\approx$3 nm length of vertically oriented T7 molecules.

Guidelines for molecular design are especially useful if the microstructure that results from a specific primary chemical structure can be correlated to performance in devices. The saturation field-effect hole mobility of T7 is strongly correlated to its molecular orientations determined from NEXAFS and its surface morphology determined from AFM. The variation in field-effect mobility with treatment temperature is shown in Figure 5. As-cast, the films exhibit a low mobility of $\approx 10^{-4}$ $cm^2/(V\ s)$, which corresponds to a disordered microstructure and a surface morphology of soft, unconnected plates. At

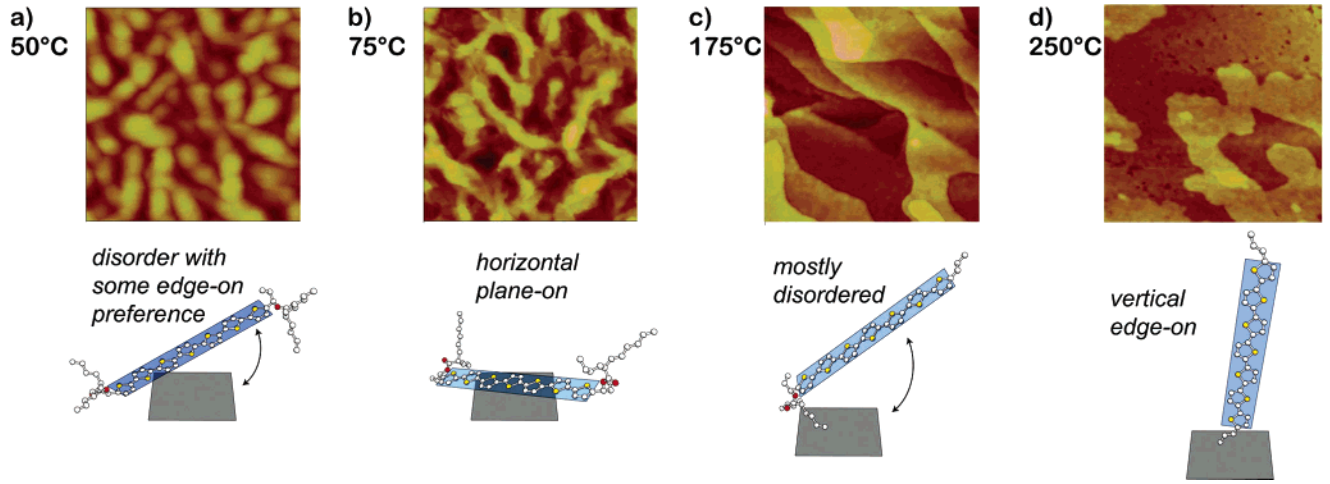

Figure 4. Variation of the T7 surface morphology with treatment temperature. AFM images are 1 μm × 1 μm and indicate height with a 20 nm range.

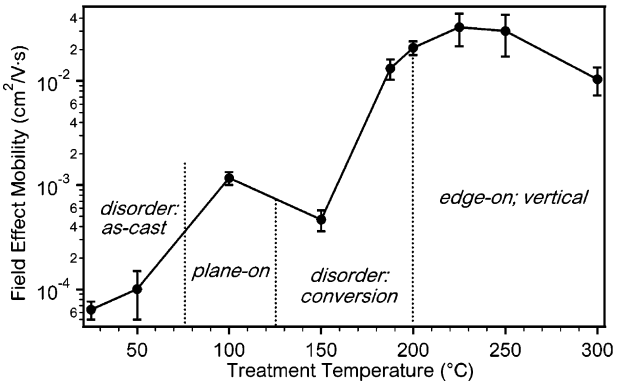

Figure 5. Variation of the T7 saturation field-effect mobility with treatment temperature.

100 °C, the mobility increases to $\approx 10^{-3}$ cm^2/(V s), which corresponds to a more ordered horizontal orientation and a surface morphology of continuous ribbons. At partial conversion, the mobility decreases again by half, which corresponds to transitional disorder and soft terraces. At full conversion, the mobility achieves its maximum of ≈ 0.04 cm^2/(V s), which corresponds to the strong vertical orientation and sharp terraces of the product. The mobility decrease at 300 °C is far less than that for T6,[24] indicating less loss of coverage and film continuity, which are consistent with the persistent molecular ordering observed with NEXAFS even at the highest temperatures.

For these oligothiophenes, ordered microstructures perform better in field-effect transistors than disordered microstructures, even if their π overlap direction is not in the film plane. The highly oriented horizontal pre-T7 phase at 100 °C exhibits higher hole mobility than either the disordered as-cast phase or the disordered transition phase. The oriented domains within the continuous ribbon network allow more efficient carrier transport.

Conclusion

Convertible oligothiophene precursors provide a unique comparison of microstructure effects caused by branched vs linear end groups. The precursors with bulky, branched end groups exhibit a dependence of microstructure on core length, whereas the products with small, linear end groups do not. The dependence on core length of the precursors may be caused by interplay between the packing forces of π affinity and phase segregation. A packing mismatch between the cores and the branched end groups may cause the septithiophene precursor to pack with its core parallel to the substrate plane. Future work will examine the effects of replacing the oligothiophene core with other aromatic moieties to change the packing force of π affinity without significantly altering molecular dimensions.

Acknowledgment. The authors thank R. J. Kline and S. Sambasivan of NIST for useful discussions. This work was supported in part by the Director, Office of Science, Office of Basic Energy Sciences, and the Division of Materials Sciences and Engineering of the U.S. Department of Energy under Contract No. DE-AC03-76SF00098.

References and Notes

(1) Katz, H. E.; Bao, Z. *J. Phys. Chem. B* **2000,** *104*, 671.
(2) Bredas, J. L.; Beljonne, D.; Cornil, J.; Calbert, J. P.; Shuai, Z.; Silbey, R. *Synth. Met.* **2001**, *125*, 107.
(3) Cornil, J.; Beljonne, D.; Calbert, J. P.; Bredas, J. L. *Adv. Mater.* **2001**, *13*, 1053.
(4) Shtein, M.; Mapel, J.; Benziger, J. B.; Forrest, S. R. *Appl. Phys. Lett.* **2002**, *81*, 268.
(5) Kelley, T. W.; Boardman, L. D.; Dunbar, T. D.; Muyres, D. V.; Pellerite, M. J.; Smith, T. Y. P. *J. Phys. Chem. B* **2003**, *107*, 5877.
(6) Genzer, J.; Kramer, E. J.; Fischer, D. A. *J. Appl. Phys.* **2002**, *92*, 7070.
(7) Ivanco, J.; Krenn, J. R.; Ramsey, M. G.; Netzer, F. P.; Haber, T.; Resel, R.; Haase, A.; Stadlober, B.; Jakopic, G. *J. Appl. Phys.* **2004**, *96*, 2716.
(8) Yang, H. C.; Shin, T. J.; Ling, M. M.; Cho, K.; Ryu, C. Y.; Bao, Z. N. *J. Am. Chem. Soc.* **2005**, *127*, 11542.
(9) Dimitrakopoulos, C. D.; Brown, A. R.; Pomp, A. *J. Appl. Phys.* **1996**, *80*, 2501.
(10) Katz, H. E.; Lovinger, A. J.; Laquindanum, J. G. *Chem. Mater.* **1998**, *10*, 457.
(11) Li, W. J.; Katz, H. E.; Lovinger, A. J.; Laquindanum, J. G. *Chem. Mater.* **1999**, *11*, 458.
(12) Meng, H.; Zheng, J.; Lovinger, A. J.; Wang, B. C.; Van Patten, P. G.; Bao, Z. N. *Chem. Mater.* **2003**, *15*, 1778.
(13) Nagamatsu, S.; Kaneto, K.; Azumi, R.; Matsumoto, M.; Yoshida, Y.; Yase, K. *J. Phys. Chem. B* **2005**, *109*, 9374.
(14) Servet, B.; Horowitz, G.; Ries, S.; Lagorsse, O.; Alnot, P.; Yassar, A.; Deloffre, F.; Srivastava, P.; Hajlaoui, R.; Lang, P.; Garnier, F. *Chem. Mater.* **1994**, *6*, 1809.
(15) Anthony, J. E.; Brooks, J. S.; Eaton, D. L.; Parkin, S. R. *J. Am. Chem. Soc.* **2001**, *123*, 9482.
(16) Payne, M. M.; Parkin, S. R.; Anthony, J. E.; Kuo, C. C.; Jackson, T. N. *J. Am. Chem. Soc.* **2005**, *127*, 4986.
(17) Meng, H.; Bendikov, M.; Mitchell, G.; Helgeson, R.; Wudl, F.; Bao, Z.; Siegrist, T.; Kloc, C.; Chen, C. H. *Adv. Mater.* **2003**, *15*, 1090.
(18) Moon, H.; Zeis, R.; Borkent, E. J.; Besnard, C.; Lovinger, A. J.; Siegrist, T.; Kloc, C.; Bao, Z. N. *J. Am. Chem. Soc.* **2004**, *126*, 15322.
(19) Curtis, M. D.; Cao, J.; Kampf, J. W. *J. Am. Chem. Soc.* **2004**, *126*, 4318.
(20) Murphy, A. R.; Frechet, J. M. J.; Chang, P.; Lee, J.; Subramanian, V. *J. Am. Chem. Soc.* **2004**, *126*, 11750.

(21) Murphy, A. R.; Chang, P. C.; VanDyke, P.; Liu, J.; Frechet, J. M. J.; Subramanian, V.; DeLongchamp, D. M.; Sambasivan, S.; Fischer, D. A.; Lin, E. K. *Chem. Mater.* **2005**, *17*, 6033.

(22) Subramanian, V.; Frechet, J. M. J.; Chang, P. C.; Huang, D. C.; Lee, J. B.; Molesa, S. E.; Murphy, A. R.; Redinger, D. R. *Proc. IEEE* **2005**, *93*, 1330.

(23) Stöhr, J. *NEXAFS Spectroscopy*; Springer-Verlag: Berlin, 1992.

(24) DeLongchamp, D. M.; Sambasivan, S.; Fischer, D. A.; Lin, E. K.; Chang, P.; Murphy, A. R.; Frechet, J. M. J.; Subramanian, V. *Adv. Mater.* **2005**, *17*, 2340.

(25) Garnier, F.; Yassar, A.; Hajlaoui, R.; Horowitz, G.; Deloffre, F.; Servet, B.; Ries, S.; Alnot, P. *J. Am. Chem. Soc.* **1993**, *115*, 8716.

(26) Katz, H. E.; Laquindanum, J. G.; Lovinger, A. J. *Chem. Mater.* **1998**, *10*, 633.

(27) Ackermann, J.; Videlot, C.; Dumas, P.; El Kassmi, A.; Guglielmetti, R.; Safarov, V. *Org. Electron.* **2004**, *5*, 213.

(28) Outka, D. A.; Stöhr, J. *J. Chem. Phys.* **1988**, *88*, 3539.

(29) DeLongchamp, D. M.; Lin, E. K.; Fischer, D. A. *Proc. SPIE* **2005**, *5940*, 54.

(30) Lovinger, A. J.; Davis, D. D.; Dodabalapur, A.; Katz, H. E.; Torsi, L. *Macromolecules* **1996**, *29*, 4952.

(31) Lovinger, A. J.; Davis, D. D.; Dodabalapur, A.; Katz, H. E. *Chem. Mater.* **1996**, *8*, 2836.

(32) Facchetti, A.; Deng, Y.; Wang, A. C.; Koide, Y.; Sirringhaus, H.; Marks, T. J.; Friend, R. H. *Angew. Chem., Int. Ed.* **2000**, *39*, 4547.

(33) Katz, H. E. *J. Mater. Chem.* **1997**, *7*, 369.

(34) Porzio, W.; Destri, S.; Mascherpa, M.; Bruckner, S. *Acta Polymerica* **1993**, *44*, 266.

(35) Schenning, A.; Kilbinger, A. F. M.; Biscarini, F.; Cavallini, M.; Cooper, H. J.; Derrick, P. J.; Feast, W. J.; Lazzaroni, R.; Leclere, P.; McDonell, L. A.; Meijer, E. W.; Meskers, S. C. J. *J. Am. Chem. Soc.* **2002**, *124*, 1269.

(36) Samori, P.; Francke, V.; Mullen, K.; Rabe, J. P. *Chem.—Eur. J.* **1999**, *5*, 2312.

(37) Kline, R. J.; McGehee, M. D.; Kadnikova, E. N.; Liu, J. S.; Frechet, J. M. J.; Toney, M. F. *Macromolecules* **2005**, *38*, 3312.